DONNAN POTENTIALS FROM STRIATED MUSCLE LIQUID CRYSTALS

Lattice Spacing Dependence

ROBERT A. ALDOROTY, NIRA B. GARTY, AND ERNEST W. APRIL
Department of Anatomy and Cell Biology, College of Physicians & Surgeons of Columbia University, New York, New York 10032

ABSTRACT Electrochemical potentials were measured as a function of myofilament packing density in crayfish striated muscle. The A-band striations are supramolecular smectic B_1 lattice assemblies of myosin filaments and the I-band striations are nematic liquid crystals of actin filaments. Both A- and I-bands generate potentials derived from the fixed charge that is associated with structural proteins. In the reported experiments, filament packing density was varied by osmotically reducing lattice volume. The electrochemical potentials were measured from the A- and I-bands in the relaxed condition over a range of lattice volumes. From the measurements of relative cross-sectional area, unit-cell volume (obtained by low-angle x-ray diffraction) and previously determined effective linear charge densities (Aldoroty, R. A., N. B. Garty, and E. W. April, 1985, *Biophys. J.*, 47:89–96), Donnan potentials can be predicted for any amount of compression. In the relaxed condition, the predicted Donnan potentials correspond to the measured electrochemical potentials. In the rigor condition, however, a net increase in negative charge associated with the myosin filament is observed. The predictablity of the data demonstrates the applicability of Donnan equilibrium theory to the measurement of electrochemical potentials from liquid-crystalline systems. Moreover, the relationship between filament spacing and the Donnan potential is consistent with the concept that surface charge provides the necessary electrostatic force to stabilize the myofilament lattice.

INTRODUCTION

Electrochemical measurements of Donnan potentials generated by the myofilament lattice were made from crayfish muscle in the relaxed condition over a range of unit-cell volumes. The fixed charge on the myosin filaments and actin filaments, which compose the myofilament lattice, causes an unequal distribution of diffusible anions and cations between the lattice and bathing medium, thereby producing a Donnan potential.

Measurements of electrochemical potential have been reported for skeletal muscle fibers that have had the cell membrane disrupted (Aldoroty and April, 1981, 1982, 1984, 1985); Aldoroty et al., 1985; April and Aldoroty, 1986; Bartels and Elliott, 1980, 1981*a,b*, 1982, 1985; Bartels et al., 1980; Chichibu, 1961; Collins and Edwards, 1971; Dewey et al., 1982; Elliott et al., 1984, 1986; Hinke, 1980; Naylor and Merrillees, 1964; Naylor et al., 1985; Pemrick and Edwards, 1974). In previous papers we have provided evidence that these electrochemical potentials are Donnan potentials (Aldoroty et al., 1985; Aldoroty and April, 1984). Data presented in this paper continue to support the hypothesis that Donnan equilibrium theory applies to both the A-band and I-band lattices of striated muscle and measurements of these potentials enable the calculation of the effective charge density within the unit cell of the myofilament lattice.

The experimental model is the myosin-filament lattice of long-tonic fibers from crayfish leg muscles. Crayfish myosin filaments, ~4.5 μm long and 18 nm in diameter (April and Wong, 1976; April, 1969), are hexagonally packed and suspended in an aqueous ionic medium. Another filament population, composed mainly of the protein actin, interdigitates the myosin-filament lattice from both ends in an approximate 6:1 (actin filament/myosin filament) unit-cell ratio. Crayfish actin filaments are ~3.6 μm long and 8 nm in diameter (April, 1969). The degree of actin-filament interdigitation into the myosin-filament lattice can be altered by stretching the muscle. The repetitive sequence of smectic myosin-filament lattices (the aniostropic A-bands) and the intervening actin filaments (the isotropic I-bands) forms the basic structure of skeletal muscle. The A-band striations are smectic B_1 liquid crystalline arrays of myosin filaments and the

Dr. Aldoroty's present address is Department of Surgery, The Mount Sinai Medical Center, New York, New York.

Dr. Garty's present address is the Department of Hormone Research, The Weizmann Institute of Science, Rehovot, Israel.

Send reprint requests to Dr. April.

I-band striations are nematic liquid crystalline assemblies of actin filaments (April, 1975*a,b*; Elliott and Rome, 1969).

The isoelectric point of crayfish myosin filaments is ~pH 4.4 (April, 1978; April et al., 1972). Therefore, at physiological pH and under the experimental conditions, the myofilaments carry a net negative charge. The surface charges generate negative electrochemical potentials of Donnan origin. Here electrochemical potentials are measured from the A-band and I-band regions of crayfish striated muscle in the relaxed condition as a function of lattice spacing. The lattices are compressed uniformly by osmotically extracting water. This is accomplished with a neutral water-soluble polymer, polyvinylpyrrolidone, which is impermeable to the lattices (Hawkins and April, 1981; Maughan and Godt, 1979, 1981). It is predicted from Donnan theory that the measured potential will become more negative as the concentration of myosin filaments and actin filaments in the lattice increases with lattice compression. This report demonstrates that the system can be described well by Donnan equilibrium theory.

MATERIALS AND METHODS

All experiments were performed on long-tonic fibers from the carpodite extensor muscle of crayfish (*Orconectes*). The dissections followed methods previously described (Aldoroty and April, 1984). Single muscle fibers, 100–200 μm in diameter, were transferred from crustacean saline solution (van Harreveld, 1936) to a crustacean relaxing solution (Table I). After mechanical skinning, the fibers were immersed in 1.0 ml/dl Triton X-100 in crustacean relaxing solution for 30 min to remove internal membranous structures (Aldoroty and April, 1984) then thoroughly washed with crustacean relaxing solution.

The physiologic conditions necessary for the maintenance of the relaxed and rigor conditions in long-tonic crayfish striated muscle fibers have been determined (Kawai and Brandt, 1976). The relaxed condition was insured by the composition of the relaxing solution, which contained an excess of Mg-ATP, and by frequently changing the relaxing solution; no experiment proceeded beyond 6 h. The rigor condition (a state of interaction between myosin filaments and actin filaments) was induced by changing the bathing medium from relaxing solution to rigor solution (Table I) with multiple washings. According to April and Schreder (1979), at 9.7 μm sarcomere length (44% overlap) rigor is accompanied by a decrease of the fiber volume by 11% relative to the relaxed condition. The onset of rigor was confirmed by measuring a decrease in fiber diameter.

TABLE I
PREPARATION OF RELAXING AND RIGOR SOLUTIONS AT pH = 7.4

Component	Concentrations	
	Relax	Rigor
	mmol/liter	
Potassium propionate	173	170
Tris	5	5
$MgCl_2$	1.12	0
Na_2H_2ATP	2	0
H_4EGTA	5	0
H_4EDTA	0	10

Tris [Tris(hydroxymethyl)aminomethane]; H_4EGTA [ethylene glycol-bis-(β-amino-ethyl ether) *N,N'*-tetraacetic acid]; and H_4EDTA (ethylene diamine -*N,N,N*±,*N'*-tetraacetic acid) (Kawai and Brandt, 1976).

Polyvinylpyrrolidone (PVP) was dissolved in relaxing solution. Polyvinylpyrrolidones of two different mass-averaged molecular masses (10,000 and 360,000 g/mol, Sigma Chemical Co., St. Louis, MO) were used to compress the skinned muscle fiber lattices osmotically (Hawkins and April, 1981; April, 1980; April and Schreder, 1979; Maughan and Godt, 1979, 1981; Millman and Wakabyashi, 1979).

Measurements of Fiber Diameter and Sarcomere Length

Fiber diameter was measured using a filar micrometer mounted in the optical system of the inverted microscope (Blinks, 1965). The magnification via this optical pathway was 200. Sarcomere length was adjusted with a micromanipulator to 9.7 μm and was monitored using light diffraction (He-Ne laser, 0.3 mW, λ = 0.6328 μm, Spectra Physics, Inc., Mountain View, CA) (April et al., 1971).

Measurements of the Myosin-Filament Lattice Plane Spacing

Measurements of the myosin filament, $d_{(1,0)}$, lattice spacing in the A-band were made by x-ray diffraction (April and Wong, 1976; April et al., 1971). Fibers were mounted in a low-angle camera of modified Franks design (April et al., 1971); sarcomere length was adjusted with a micromanipulator to 9.7 μm using light diffraction. The x-ray source was the Cu Kα peak from a microfocus rotating anode x-ray generator (Elliott GX 6; Marconi Avionics Ltd., Borhamwood, England) operated at 35 kV and 22 mA. A one-dimensional position sensitive detector (PSD 1000; Tennelec Inc., Oak Ridge, TN) collected the diffraction patterns in ~15 min. The specimen-to-detector distance was equivalent to 16,017 channels (7.5×10^{-3} mm/channel). The diffraction patterns were analyzed by computer (Minc 11/23; Digital Equipment Corp., Marlboro, MA) with programs developed in this laboratory.

Measurements of Electrochemical Potential

The preparations were mounted on the stage of an inverted microscope (Nikon M2; Ehrenrich Photo-optical Corp., Garden City, NY) equipped with polarizing optics. A magnification of 600 provided a clear view of the A- and I-bands. Sarcomere length was adjusted with a micromanipulator to 9.7 μm and was monitored using light diffraction as previously discussed (Aldoroty and April, 1984).

Measurements of electrochemical potentials were made using 3 mol/liter KCl filled microelectrodes with an outer tip diameter of 0.3–0.4 μm (Aldoroty and April, 1984). All electrodes had resistances from 10 to 15 MΩ. Electrode resistance was monitored by passing current such that 1 mV was equivalent to 1 MΩ. An Ag/AgCl electrode provided continuity between the fluid phase within the glass microelectrode and the positive terminal of the preamplifier (model NF1; Bioelectronics Bioelectric Instruments, Hastings-on-Hudson, NY). The reference electrode consisted of a 3.0 g/dl agar-salt bridge filled with 3 mol/liter KCl in series with an Ag/AgCl electrode in 3 mol/liter KCL and connected to the common terminal of the preamplifier. Measurements were recorded on a chart recorder (Brush 2200 series with a medium gain DC preamplifier, model 13-461510, Gould Inc., Cleveland, OH). The entire apparatus was protected from random radio frequency by appropriate screening and grounding (Aldoroty and April, 1984).

The technique and theory for using microelectrodes to measure the electrochemical potentials generated by fixed charge along the myofilaments has been discussed previously (Aldoroty et al., 1985; Aldoroty and April, 1984; Elliott and Bartels, 1982; Naylor, 1981; Overbeek, 1956).

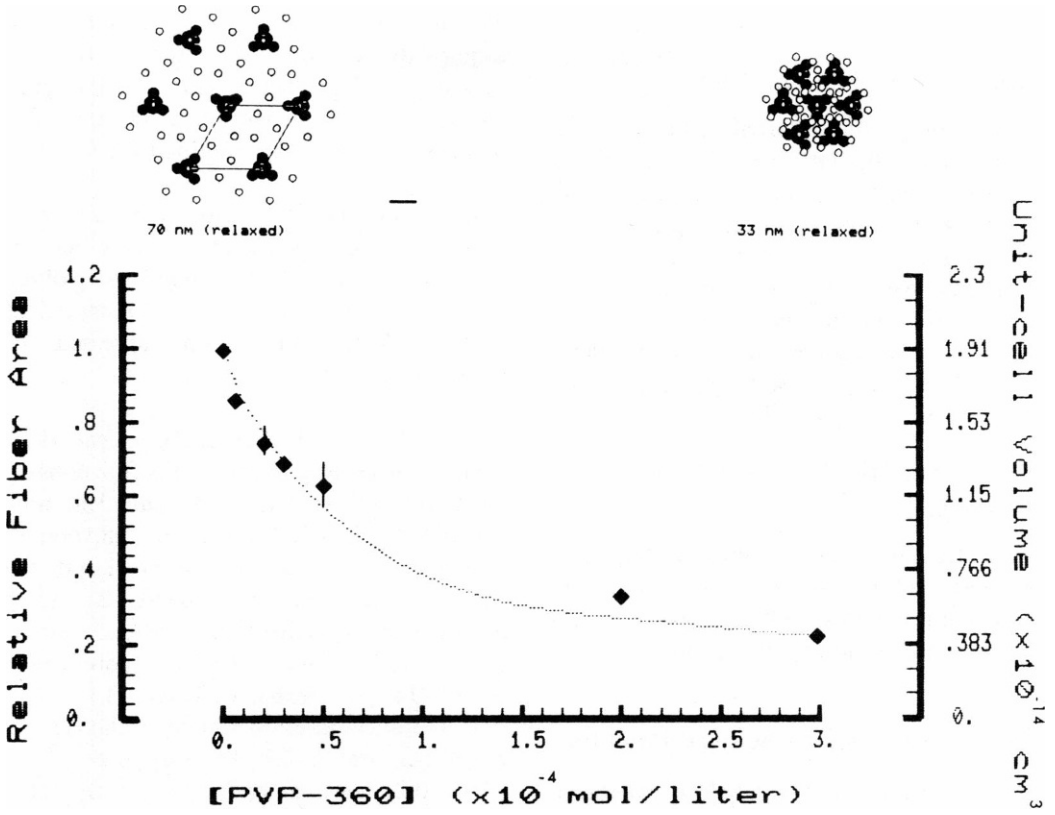

FIGURE 1 Fiber area as a function of osmotic compression. Relative skinned fiber area and corresponding unit-cell volume are plotted as a function of PVP-360 concentration in the bathing medium. The data points are represented by diamonds with the standard deviations from the means indicated by bars. The curve is a spline-fit to theoretical points determined according to the method of Hawkins and April (1983). Computer-generated schematic representations of the overlap region of the A-band lattice of crayfish are indicated for the uncompressed condition (*left*) and 80% compression (*right*). The 6:1 unit cell is indicated. Bar, 25 nm.

TABLE II
EXPERIMENTAL RESULTS AND STATISTICS

Condition	[PVP-360]	A/A_0		A-Band		I-Band	
		Measured	Predicted	$\langle\psi_D\rangle$	n	$\langle\psi_D\rangle$	n
Relaxed	*mol/liter*			*mV*		*mV*	
(2)	0	1.00	1.00	−1.71 ± 0.24	22	−0.71 ± 0.16	11
(1)	5.0×10^{-6}	0.86	0.92	−2.02 ± 0.28	19	−1.39 ± 0.25	11
(1)	2.0×10^{-5}	0.77	0.78	−1.91 ± 0.19	14	−1.31 ± 0.13	7
(1)	2.0×10^{-5}	0.72	0.78	−1.95 ± 0.20	15	−1.15 ± 0.22	23
(1)	3.0×10^{-5}	0.69	0.69	−2.41 ± 0.31	15	−1.65 ± 0.31	4
(1)	5.0×10^{-5}	0.68	0.57	−2.07 ± 0.41	26	−1.24 ± 0.24	29
(1)	5.0×10^{-5}	0.65	0.57	−2.62 ± 0.34	23	−1.35 ± 0.27	13
(1)	5.0×10^{-5}	0.57	0.57	−2.58 ± 0.42	12	−1.60 ± 0.26	8
(1)	1.0×10^{-4}*	0.50	0.50	−3.15 ± 0.74	22	−2.00 ± 0.56	15
(1)	2.0×10^{-4}	0.33	0.27	−5.34 ± 0.98	44	−2.34 ± 1.09	48
(1)	3.0×10^{-4}	0.22	0.22	−8.28 ± 1.52	29	−3.56 ± 0.83	16
Rigor							
(5)	0	0.89	—	−2.18 ± 0.33	88	−0.89 ± 0.22	25

A/A_0 is the relative fiber area; $\langle\psi_D\rangle$ is the mean measured potential; ± is the standard deviation of the measurements of potential; n is the number of measurements of the potential; and * indicates that PVP-10 was used to compress the lattice.

RESULTS

Measurements of Fiber Diameter

The effect of osmotic compression exerted by impermeant polymers upon the skinned fiber lattice has been described (Hawkins and April, 1981, 1983). The measurements of fiber diameter were made at the sarcomere length 9.7 μm. At this sarcomere length, each half I-band is 2.5 μm and the overlapped portion at each end of the A-band is 1.1 μm (the A-band length is 4.5 μm and the Z-line is 0.2 μm). Skinned-fiber relative cross-sectional areas were calculated and are plotted against PVP-360 concentration in Fig. 1. The data are summarized in Table II.

Measurements of the Myosin-Filament Lattice Spacing

Low-angle x-ray diffraction measurements of the $d_{(1,0)}$ spacing in the relaxed condition with no osmotic compression and at a sarcomere length of 9.7 μm gave a $d_{(m,m)}$, myosin-filament interaxial spacing, of 70 nm (SD = 3 nm).

Measurements of Electrochemical Potential

A-band. The measured A-band electrochemical potentials are plotted as a function of fiber relative cross-sectional area and unit-cell volume in Fig. 2. Upon osmotic compression of the relaxed A-band, the unit-cell volume decreases and the equivalent fixed charge concentration increases. The measured electrochemical potentials become more negative, ranging from -1.71 to -8.28 mV (Table II).

In the uncompressed A-band in the rigor condition, the mean measured electrochemical potential was -2.18 mV (SD = 0.33 mV), which is significantly different from the mean measured electrochemical potential of -1.71 mV (SD = 0.24 mV) in the uncompressed A-band in the relaxed condition.

I-band. In Fig. 2, the measured I-band electrochemical potentials are plotted as functions of fiber relative cross-sectional area and an equivalent unit-cell volume calculated from the A-band unit-cell volume (Aldoroty et al., 1985). Upon osmotic compression of the I-band, the equivalent unit-cell volume decreases and the equivalent fixed charge concentration increases. The measured electrochemical potentials become more negative, ranging from -0.71 to -3.56 mV (Table II).

In the uncompressed I-band in the rigor condition, the mean measured electrochemical potential was -0.89 mV (SD = 0.22 mV), which is significantly different from the mean measured electrochemical potential of -0.71 mV

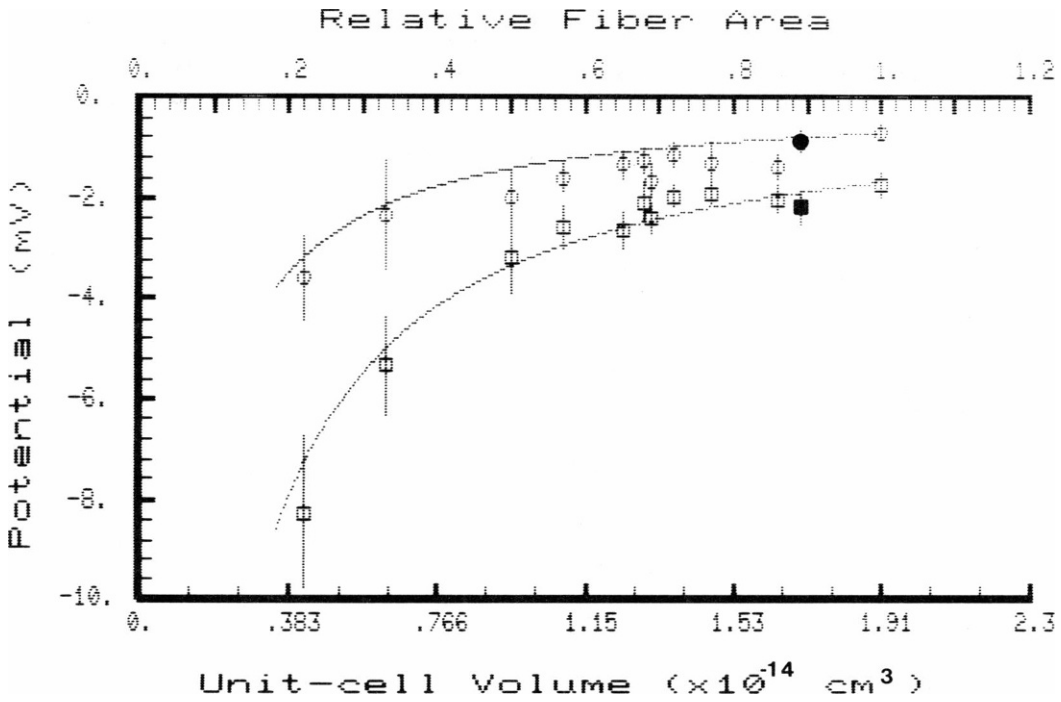

FIGURE 2 Potential as a function of relative fiber area and unit-cell volume. The measured potentials from the A-band (open squares) and the I-band (open circles) regions in the relaxed condition as well as the measured potentials from the A-band (filled squares) and the I-band (filled circles) regions in the rigor condition are plotted against both the relative fiber area and the corresponding unit-cell volume. The bars indicate standard deviations from the means. The relaxed A-band data approximate a curve predicted from Donnan theory. This curve also coincides with a curve calculated from April and Wong (1976). The relaxed I-band data approximate a curve predicted from Donnan theory with a unit-cell filament ratio of 5.1:1 (Aldoroty et al., 1985). The A-band rigor point is significantly different from the predicted curve; the I-band rigor point does not appear to be significantly different from the predicted curve.

(SD = 0.16 mV) in the uncompressed A-band in the relaxed condition.

ANALYSIS

Resolution of Measured Electrochemical Potentials with Donnan Theory (Relaxed Condition)

A-band. The unit-cell volume of the A-band myosin-filament lattice was calculated according to:

$$V = l_m \frac{d_{(1,0)}^2}{\sin(60°)}, \tag{1a}$$

where l_m represents the length of a myosin filament or A-band and $d_{(1,0)}$ is the lattice plane spacing (Hawkins and April, 1981). Interaxial myosin-filament spacings, $d_{(m,m)}$, were calculated from

$$d_{(m,m)} = \frac{d_{(1,0)}}{\sin(60°)} \tag{1b}$$

(April et al., 1971). Hence, 70 nm $d_{(m,m)}$ spacing is equivalent to an A-band unit-cell volume of 1.9×10^{-14}cm^3.

For this experimental system, relative unit-cell areas calculated from low-angle x-ray measurements of spacings of the $d_{(1,0)}$ lattice planes are equivalent to relative fiber areas calculated from light microscopic measurements of the fiber diameter (Hawkins and April, 1981, 1983). Since the length of a myosin filament is constant, it is possible to calculate absolute unit-cell volumes of the A-band. The empirical expression is

$$V = (A/A_0)(V_0), \tag{2}$$

where A/A_0 is the relative fiber area and V_0 is the unit-cell volume calculated from Eq. 1a. The correlation between relative fiber area and A-band unit-cell area and volume is illustrated in Fig. 1. The sum of the unit-cell areas must equal the total fiber cross-sectional area because the contribution by the sarcoplasmic reticulum to cross-sectional area has been removed completely by treating the fiber with Triton X-100, a non-ionic detergent (Aldoroty and April, 1984).

The molar concentration of the filaments is given by

$$C_z = \frac{n}{VN}, \tag{3}$$

where n is the number of filaments in the unit cell, V is the unit-cell volume in liters, and N is Avogadro's number. The charge concentration attributable to the protein in the A-band is calculated from

$$\Gamma = zC_z, \tag{4}$$

where z is the unit charge on the protein with a molar concentration C_z. According to Benedek and Villars (1979) the Donnan potential is

$$\psi_D = \frac{kT}{e} \ln\left(\sqrt{1 + \frac{\Gamma^2}{4C^2}} - \frac{\Gamma}{2C}\right), \tag{5}$$

where ψ_D is the Donnan potential, k is the Boltzmann constant, T is the temperature in degrees Kelvin, e is the charge on an electron, and C is the concentration of univalent mobile ions in the external phase. A derivation and discussion of this equation as it applies to this experimental system has been presented in a preceding paper (Aldoroty et al., 1985).

The concentrations of the dissociated Tris buffer and the potassium propionate were calculated using the Henderson-Hasselbach equation (pK = 4.9 for potassium propionate and pK = 8.2 for Tris buffer) (Weast, 1972; Segal, 1968). Other free multivalent ion concentrations of the relaxing solution and the rigor solution were calculated using a set of FORTRAN programs developed by P. W. Brandt. A general equation for the Donnan potential which accounts for multivalent diffusible ions, as described by Naylor (1977, 1985), was used to determine charge density. Thus, Eq. 5 becomes

$$\Gamma = \sum_i z_i c_i \exp\left(\frac{-z_i e \psi_D}{kT}\right), \tag{6}$$

where z_i is the charge on the ith diffusible ion with concentration c_i in the external phase. This departure from our previous work (Aldoroty et al., 1985), in which free multivalent ions were accounted for as mole equivalents of charge, provides more accurate values of the charge densities along the filaments.

The A- and I-band each are treated as a single ionic phase (Hawkins and April, 1981, 1983; April, 1978; Elliott, 1973). Further, the charge along the myosin filaments and actin filaments are assumed to be distributed evenly along the length of the filaments and in the plane perpendicular to the filaments. This assumption is reasonable considering the microenvironment that the microelectrode samples (Elliott and Bartels, 1982). Hence, it is possible to derive fixed-charge concentration (mol e^-/liter) and effective linear-charge densities (e^-/μm) for the unit-cell, myosin filament, and actin filament as detailed in a previous paper (Aldoroty et al., 1985). From the measured A-band potential (−1.71 mV) and unit-cell volume of the noncompressed A-band in the relaxed condition as well as Eqs. 3, 4, and 6, an effective unit-cell linear charge density of 6.6×10^4 e^-/μm is calculated. From this charge density a theoretical Donnan potential curve is plotted as a function of relative unit-cell volume (Fig. 2).

Further, the unit-cell charge density at a sarcomere length of 9.7 μm can be reconstructed from the charge contributions of the myosin filaments and the variably interdigitating actin filaments. The linear charge densities of the myosin filament, 7.1×10^4 e^-/μm, and actin filament, 7.4×10^3 e^-/μm, have been determined (recal-

culated from Aldoroty et al., 1985). (It should be noted that when multivalent ions were accounted fully, the myosin-filament charge density changed from 6.6×10^4 to 7.1×10^4 $e^-/\mu m$, while the actin-filament charge density changed from 6.8×10^3 to 7.4×10^3 $e^-/\mu m$.) As such, an effective A-band unit-cell linear charge density of 6.5×10^4 $e^-/\mu m$ is predicted for a sarcomere length of 9.7 μm. From Eqs. 3, 4, and 6, this A-band unit-cell effective linear charge density corresponds to a Donnan potential of -1.70 mV. This calculated Donnan potential is within one standard deviation of the measured electrochemical potential (-1.71 ± 0.24 mV).

Finally, the number of electrons per unit cell and the moles of electrons per unit cell are plotted against unit-cell volume in Fig. 3. The progression of calculations is summarized in Table IIIA. The standard deviations were calculated using compounding of error theory (Wilson, 1952). The slope (0.0029 mol e^-/liter) is not significantly different from zero ($P = 0.1992$). This indicates that the number of electrons within the unit cell due to the myosin filaments and actin filaments is constant throughout the range of osmotic compression. Thus, one of the requisite assumptions for the application of Donnan theory to this sytem is substantiated.

I-band. In a similar manner, an analysis may be made for the I-band in the relaxed condition, using Eq. 3 where $n = 5.1$ (Aldoroty et al., 1985). The actin concentration in the I-band can be determined from the linear charge density of the actin filament, 7.4×10^3 $e^-/\mu m$ (recalculated from Aldoroty et al., 1985). This can be applied to any sarcomere length to calculate the effective unit-cell linear charge density of the I-band (Aldoroty et al., 1985). The calculated I-band unit-cell effective linear charge density (2.8×10^4 $e^-/\mu m$) corresponds to a Donnan potential of -0.70 mV. This predicted Donnan potential nearly equals the measured electrochemical potential (-0.71 ± 0.16 mV). Using the linear charge density calculated from the measured electrochemical potential, a theoretical Donnan potential curve is derived and plotted as a function of unit-cell volume (Fig. 2).

Finally, the number of electrons per equivalent I-band unit cell and the moles of electrons per equivalent I-band unit cell are plotted against equivalent unit-cell volume in Fig. 3 and the calculations are summarized in a step-wise manner in Table IIIB. The standard deviations were calculated using compounding-of-error theory (Wilson, 1952). The slope (0.0019 mol e^-/liter) is not significantly different from zero ($P = 0.7192$), indicating that the number of electrons of charge in the equivalent I-band unit-cell during osmotic compression remains constant. Again, this substantiates the assumption that charge remains constant during compression, an assumption necessary for the application of Donnan theory to this system.

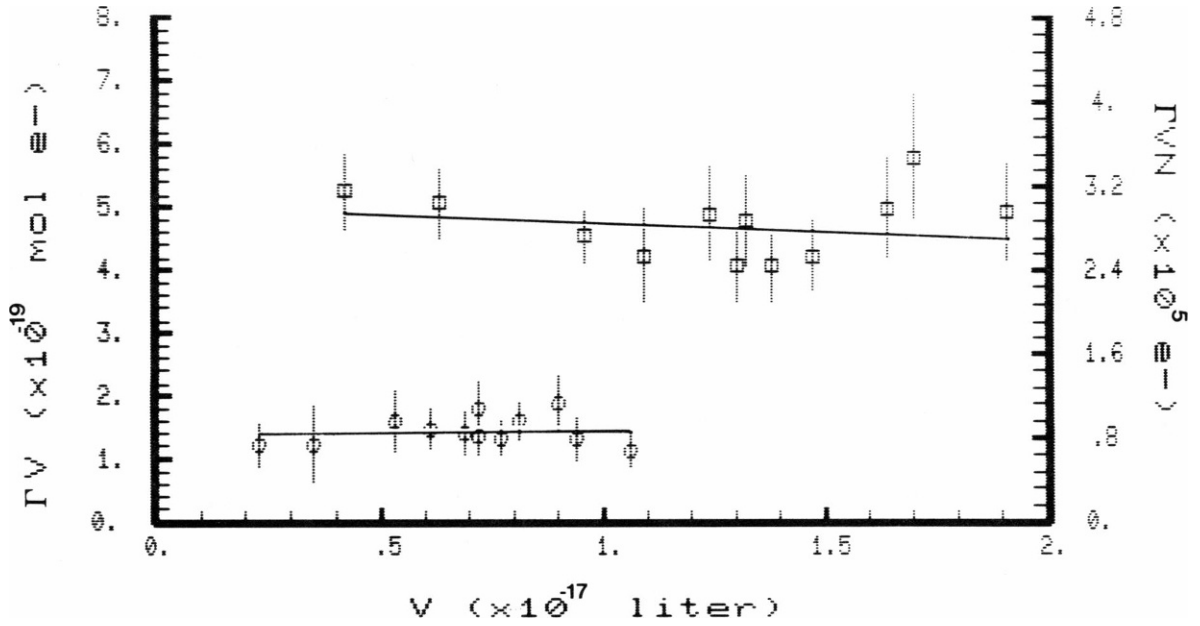

FIGURE 3 Charge per unit cell as a function of unit-cell volume. The moles of electrons per unit cell (ΓV) and the number of electrons per unit cell (ΓVN) are plotted against the unit-cell volume for the A-band (open squares) and the I-band (open circles) both in the relaxed condition at a sarcomere length of 9.7 μm. The slope of each data set is essentially zero, indicating that the filament charge is constant during osmotic compression. The linear regression constants for the A-band are: slope = 0.0029 mol e^-/liter and y-intercept = 5.00×10^{-19} mol e^-. Using a t test and a zero slope as the null hypothesis, the probability of there being no difference falls within the acceptance area ($0.05 \leq 0.1992 \leq 0.95$), verifying the hypothesis that there is no significant difference between the linear regression slope of the A-band data and zero. The linear regression constants for the I-band are: slope = 0.0019 mole e^-/liter and y-intercept = 1.34×10^{-19} mol e^-. Similarly, the probability of there being no difference falls within the acceptance area ($0.05 \leq 0.7192 \leq 0.95$), verifying that there is no significant difference between the linear regression slope of the I-band data and zero.

TABLE IIIA
A-BAND CALCULATIONS

A/A_0	$\langle\psi_D\rangle$	Γ	V	ΓV
Relaxed	mV	$\times 10^{-2}$ mol e^-/liter	$\times 10^{-17}$ liter	$\times 10^{-19}$ mol e^-
1.00	−1.71 ± 0.24	2.59 ± 0.34	1.91 ± 0.17	4.94 ± 0.77
0.86	−2.02 ± 0.28	3.06 ± 0.40	1.64 ± 0.15	5.01 ± 0.77
0.77	−1.91 ± 0.19	2.89 ± 0.27	1.47 ± 0.14	4.24 ± 0.55
0.72	−1.95 ± 0.20	2.95 ± 0.29	1.38 ± 0.13	4.07 ± 0.54
0.69	−2.41 ± 0.31	3.64 ± 0.44	1.32 ± 0.12	4.80 ± 0.72
0.68	−2.07 ± 0.41	3.13 ± 0.59	1.30 ± 0.12	4.07 ± 0.85
0.65	−2.62 ± 0.34	3.95 ± 0.49	1.24 ± 0.11	4.91 ± 0.74
0.57	−2.58 ± 0.42	3.90 ± 0.61	1.09 ± 0.10	4.25 ± 0.75
0.50	−3.15 ± 0.74	4.75 ± 1.10	0.95 ± 0.09	4.54 ± 0.42
0.33	−5.34 ± 0.98	8.04 ± 1.40	0.63 ± 0.07	5.07 ± 0.55
0.22	−8.28 ± 1.52	12.52 ± 2.30	0.42 ± 0.50	5.26 ± 0.61
Rigor				
0.89	−2.18 ± 0.33	3.42 ± 0.47	1.70 ± 0.16	5.82 ± 0.87

A/A_0 is the relative fiber area; $\langle\psi_D\rangle$ is the mean measured potential; Γ is the concentration of electrons due to the myofilaments; V is the unit-cell volume of the A-band; and ± is the standard deviation of the corresponding measurements.

TABLE IIIB
I-BAND CALCULATIONS

A/A_0	$\langle\psi_D\rangle$	Γ	V	ΓV
Relaxed	mV	$\times 10^{-2}$ mol e^-/liter	$\times 10^{-17}$ liter	$\times 10^{-19}$ mol e^-
1.00	−0.71 ± 0.16	1.08 ± 0.23	1.06 ± 0.11	1.14 ± 0.27
0.86	−1.39 ± 0.25	2.11 ± 0.36	0.90 ± 0.09	1.89 ± 0.37
0.77	−1.31 ± 0.13	1.99 ± 0.19	0.81 ± 0.09	1.61 ± 0.23
0.72	−1.15 ± 0.22	1.74 ± 0.31	0.77 ± 0.08	1.34 ± 0.27
0.69	−1.65 ± 0.31	2.50 ± 0.44	0.72 ± 0.07	1.80 ± 0.36
0.68	−1.24 ± 0.24	1.88 ± 0.34	0.72 ± 0.07	1.35 ± 0.28
0.65	−1.35 ± 0.27	2.05 ± 0.38	0.69 ± 0.07	1.41 ± 0.30
0.57	−1.60 ± 0.26	2.42 ± 0.37	0.61 ± 0.06	1.48 ± 0.27
0.50	−2.00 ± 0.56	3.03 ± 0.80	0.53 ± 0.06	1.60 ± 0.46
0.33	−2.34 ± 1.09	3.50 ± 1.56	0.35 ± 0.04	1.34 ± 0.57
0.22	−3.56 ± 0.83	5.37 ± 1.19	0.23 ± 0.03	1.24 ± 0.31
Rigor				
0.89	−0.89 ± 0.22	1.40 ± 0.31	0.94 ± 0.10	1.32 ± 0.32

A/A_0 is the relative fiber area; $\langle\psi_D\rangle$ is the mean measured potential; Γ is the concentration of electrons due to the actin filaments; V is the unit-cell volume of the I-band (Aldoroty et al., 1985); and ± is the standard deviation of the corresponding measurements.

Resolution of Measured Electrochemical Potentials with Donnan Theory (Rigor Condition)

I-band. In the rigor condition the measured I-band potential is −0.89 mV. It has been reported that the induction of the rigor condition in crayfish long tonic fibers at a sarcomere length of 9.7 μm is accompanied by a decrease of 11% in unit-cell volume relative to the relaxed condition (April and Schreder, 1979). Based upon this simple volume effect, the I-band curve for the relaxed condition in Fig. 2 predicts an I-band potential of −0.80 mV at a relative unit-cell volume of 0.89. The measured I-band potential of −0.89 mV in the rigor condition is more negative than the predicted value. A t test (Ostle and Mensing, 1975) that compares the predicted potential (−0.80 mV) to the distribution of measured I-band rigor potentials (−0.89 mV) indicates that the difference is marginally significant ($P = 0.9742$) at the 95% confidence level. From Eq. 6, there are 3.2×10^4 $e^-/\mu m$ along the equivalent I-band unit cell and 6.2×10^3 $e^-/\mu m$ along the actin filament in the rigor condition, while 2.9×10^4 $e^-/\mu m$ along the equivalent I-band unit cell and 5.8×10^3 $e^-/\mu m$ along the actin filament was predicted from the theoretical curve in Fig. 2. However, it cannot be said with certainty that the difference between the derived linear charge density and the predicted linear charge density for the actin filament in rigor is significant.

A-band. In the rigor condition the measured A-band potential is −2.18 mV. Based upon the decrease of 11% in unit-cell volume relative to the relaxed condition (April and Schreder, 1979), the A-band curve for the relaxed condition in Fig. 2 predicts a potential of −1.89

mV. The measured A-band potential of −2.18 mV in the rigor condition is more negative than the predicted value. A t test (Ostle and Mensing, 1975) comparing the predicted potential (−1.89 mV) to the distribution of measured rigor potentials (−2.18 mV), indicates that the rigor potential measured in the A-band differs significantly from the predicted value ($P > 0.9999$). The discrepancy between the measured rigor A-band potential and the predicted rigor A-band potential indicated that the A-band potential measured in the rigor condition includes an additional factor other than the result of a pure volume effect. From Eq. 6, there are 7.7×10^4 $e^-/\mu m$ along the A-band unit cell in the rigor condition, while 6.8×10^4 $e^-/\mu m$ was predicted from the theoretical curve in Fig. 2. Hence, relative to the relaxed condition at a relative volume of 0.89, an additional 1.1×10^4 $e^-/\mu m$ are exposed in the A-band during the rigor condition. Because the actin filament charge density does not appear to change significantly during rigor, the net increase in negative charge density is attributed to the myosin filament. Therefore, the charge density of the myosin filament in rigor is 8.2×10^4 $e^-/\mu m$.

There is more than one possible interpretation of the rigor data. However, considering the geometry of interaction sites between actin filaments and myosin filaments in crayfish muscle and assuming that all of the observed increase in charge during rigor occurs at or between interaction sites, a simple caculation can reduce the difference in charge to sites within the unit cell. Based on a thick filament composed of nine cross-bridges per period (April, E. W., unpublished observations), 14.3 nm between cross-bridges, involvement of cross-bridges in the overlap zone only (1 μm on either end of the A-band at a sarcomere length of 9.7 μm), and a 5:5.1 filament ratio per unit cell (Aldoroty et al., 1985), the 1.1×10^4 $e^-/\mu m$ in rigor can be reduced to an additional 12–14 e^- per cross-bridge interaction.

DISCUSSION

The premise that osmotic compression of the myofilament lattice should produce an increase in measured electrochemical potential was tested and shown to be valid. The osmotic compression data, which represent reduction of unit-cell volume, are described well by Donnan equilibrium theory. In the control condition (no external osmotic compression), an A-band electrochemical potential of −1.71 mV was recorded. This electrochemical potential corresponds to an effective linear charge density for the A-band unit cell of 6.6×10^4 $e^-/\mu m$, using the method previously reported (Aldoroty et al. 1985). This linear charge density and Donnan theory was then used to calculate a theoretical curve relating Donnan potential to unit-cell volume. The predicted Donnan potentials correspond to measured electrochemical potentials over the range of lattice compression (Fig. 2). Previous work (Aldoroty et al., 1985) determined the linear charge densities on the myosin filaments (6.6×10^4 $e^-/\mu m$) and actin filament (6.8×10^3 $e^-/\mu m$). These values have been revised by accounting for multivalent diffusible ions so that the linear charge densities for myosin and actin filaments are 7.1×10^4 and 7.4×10^3 $e^-/\mu m$, respectively. Using these values, the effective unit-cell linear charge density of the A-band may be predicted for any sarcomere length (Aldoroty et al., 1985) or for any degree of osmotic compression. From these component effective linear charge densities, the A-band unit-cell linear charge density calculated for the experimental condition in the absence of any compression is 6.5×10^4 $e^-/\mu m$; this is equivalent to a Donnan potential of −1.70 mV. The experimentally measured value of the A-band electrochemical potential is -1.71 ± 0.23 mV; this is equivalent to an A-band unit-cell effective linear charge density of 6.6×10^4 $e^-/\mu m$. Also, from the effective linear charge density of the actin filament, the I-band equivalent unit-cell linear charge density in the absence of any compression is 2.8×10^4 $e^-/\mu m$; this is equivalent to a Donnan potential of −0.70 mV. The experimentally measured value of the I-band electrochemical potential is -0.71 ± 0.16 mV. The values are surprisingly close considering that the structure of the I-band varies from one end to the other and, as such, the equivalent I-band unit-cell volume only represents a conceptual convenience. The ability of Donnan theory to predict the A- and I-band values, based upon independently determined linear charge densities, while not conclusive, certainly is not inconsistent with the premise that the electrochemical potentials measured from the myosin-filament and actin-filament liquid-crystalline lattices are Donnan potentials.

When using Eq. 6 to predict Donnan potentials for any fixed charge concentration (varied here by osmotically adjusting the unit-cell volume), it is assumed that the charge densities along the actin and myosin filaments do not change. To verify this assumption, unit-cell charge (determined from electrochemical measurements) was plotted against unit-cell volume (Fig. 3). For both the A-band and I-band, the slopes of the regression lines fit to the data are not significantly different from zero. The zero slopes clearly indicate that there is no change in intralattice ionic strength in skinned fibers during the osmotic compression with polymer. With compression, the fixed-charge concentration within the lattice increases and perturbs the Donnan distribution of ions associated with the fixed charges (Aldoroty and April, 1982; April and Aldoroty, 1986). Calculations based on Donnan theory provide predictions of specific ion concentrations within the A-band (method of D. W. Maughan and R. E. Godt, to be published). For example, at 50% volume compression the average concentrations of the A-band univalent and divalent cations increase by factors of 1.05 and 1.12, respectively; the average concentrations of A-band univalent and divalent anions decrease by factors of 0.94 and 0.89, respectively. The computed average A-band ionic strength

TABLE IV
SUMMARY OF THE AVAILABLE EXPERIMENTAL DATA: RELAXED CONDITION pH = 7.0–7.5

Preparation	Overlap	[Charge] A-band	[Charge] I-band	Linear charge density A-band	Linear charge density Myosin filament	Linear charge density Actin filament	Method	Investigators
	%	*mmol e^-/liter*			$e^-/\mu m$			
Rat semitendinosous (glycerinated)	—	36	36	—	—	—	M*	Bartels and Elliott (1982, 1985)
Rat semitendinosous (saponin skinned)	—	70	70	—	5.9×10^4	3.0×10^4	M + L	Bartels and Elliott (1982, 1985)
Rat semitendinosous (saponin skinned and Brij treated)	—	36	36	—	—	—	M	Bartels and Elliott (1982, 1985)
Rabbit psoas	—	—	—	—	[2×10^4] to [5×10^4]	[1×10^4]	B	Elliott (1973)
Rabbit psoas (glycerinated)	56	46		—	—	—	M	Pemrick and Edwards (1974)
Rabbit psoas	—	33	32	—	—	—	M	Bartels and Elliott (1981*a*)
(glycerinated)	—	31	31	—	2.3×10^4	1.5×10^4	M + L	Bartels and Elliott (1985)
Frog semitendinosous	—	—	—	—	[5×10^4]	[5×10^3]	B	Elliott (1973)
Barnacle (mechanically skinned)	—	125	124	—	—	—	M	Bartels and Elliott (1981*b*)
Crayfish (mechanically skinned)	—	—	—	—	[17×10^4]	[1×10^4]	B	April and Wong (1976)
Crayfish (mechanically skinned)	0–100	—	—	—	[8.7×10^4]	[6.8×10^3]	L + B	April and Wong (1976)
Crayfish	44	24	10	—	—	—	M	Aldoroty and April (1984)
(mechanically skinned)	0	36	22	6.6×10^4	6.6×10^4	6.8×10^3	M + L	Aldoroty et al. (1985)
& Triton treated)	0	38	24	7.1×10^4	7.1×10^4	7.4×10^3	M + L	
	44	26	11	6.6×10^4	—	—		
	44	[26]	[13]	[6.5×10^4]	—	—		

Missing values indicate that the data was not reported. Values that are between columns indicate that no distinction was made; [ ] indicates a prediction by the investigator.
*Method key: M, microelectrode data; B, biochemcial data; L, lattice spacing data.

TABLE V
SUMMARY OF THE AVAILABLE EXPERIMENTAL DATA: RIGOR CONDITION pH = 7.0–7.5

Preparation	Overlap	[Charge] A-band	[Charge] I-band	Linear charge density A-band	Linear charge density Myosin filament	Linear charge density Actin filament	Method	Investigators
	%	*mmol e^-/liter*			$e^-/\mu m$			
Rat semitendinosous (glycerinated)	—	59	30	—	—	—	M*	Bartels and Elliott (1982, 1985)
Rat semitendinosous	—	59	30	—	—	—	M	Bartels and Elliott (1982)
(saponin skinned)	—	63	30	—	5.1×10^4	1.2×10^4	M + L	Bartels and Elliott (1985)
Rat semitendinosous (saponin skinned and Brij treated)	—	59	30	—	—	—	M	Bartels and Elliott (1982)
Rabbit psoas (glycerinated)	56	26		—	—	—	M	Pemrick and Edwards (1974)
Rabbit psoas (glycerinated)	—	137		—	8.8×10^4	1.6×10^4	M + L	Elliott et al. (1978) (see also Naylor et al, 1985)
Rabbit psoas (glycerinated)	—	—	—	—	4.6×10^4	1.1×10^4	M + L	Bartels and Elliott (1980)
Rabbit psoas (glycerinated)	—	53	29	—	4.7×10^4	1.3×10^4	M + L	Bartels and Elliott (1981*a*, 1985) Naylor et al, (1985)
Barnacle (mechanically skinned)	—	119	70	—	—	—	M	Bartles and Elliott (1981*b*)
Frog ventricle (glycerinated)	—	56		—	—	—	M	Collins and Edwards (1971)
Crayfish (mechanically skinned	44	33	13	—	—	—	M	Aldoroty and April (1984)
and Triton treated)	44	34	14	7.7×10^4	8.2×10^4	6.2×10^3	M + L	

Missing values indicate that the data was not reported. Values that are between columns indicate that no distinction was made.
*Method key: M, microelectrode data; L, lattice spacing data.

increases only by a factor of 1.03, which is considered to be insignificant (April and Maughan, 1986). Moreover, a series of experiments, beyond the scope of the present report, demonstrates that changes in ionic strength and pH alter filament charge in a predictable manner.

The linear charge densities of 7.1×10^4 and 7.4×10^3 $e^-/\mu m$ for the respective myosin and actin filaments of relaxed crayfish muscle approximate those reported in other species (Table IV). The linear charge density for the A-band of crayfish muscle in the rigor condition (7.7×10^4 $e^-/\mu m$) is comparable to other reported values (Table V). In both relaxed and rigor conditions, differences in ionic concentration, pH, relative sarcomere length, and species should affect charge. For example, most of the experiments summarized in Tables IV and V were performed at approximately one-half the ionic concentration of crayfish; the external free ion concentration is inversely proportional to the Donnan potential. These differences preclude drawing any quantitative conclusions based upon comparison of this study with those in the literature. Regardless of the differences in experimental method, our study concurs with the psoas work of Bartels and Elliott (1980, 1981*a*, 1985), Elliott et al. (1986), Naylor et al. (1985) as well as Scordilis (1975) in that induction of rigor increases myosin filament negative charge. From our observed 1.1×10^4 $e^-/\mu m$ increase in rigor charge density, the increase of 12–14 electrons per crayfish myosin cross-bridge during rigor compares favorably with the 18 additional electrons per rabbit myosin cross-bridge interaction during rigor measured by Bartels and Elliott (1985).

From low-angle x-ray diffraction data, April and Wong (1976) estimated the effective linear charge density of the myosin filament to be 8.7×10^4 $e^-/\mu m$ and the actin filament to be 6.8×10^3 $e^-/\mu m$. When their estimates of the effective charge density were adjusted to account for both the total unit-cell charge at a sarcomere length of 9.7 μm and the experimental conditions of this study, the analysis used above provides a unit-cell value of 6.1×10^4 $e^-/\mu m$. This value generates a curve that is nearly coincident to that plotted in Fig. 2. The proximity of the data points to the curve based upon the data of April and Wong (1976) substantiates their conclusion that the effective electrostatic charge in the A-band unit cell of skinned crayfish muscle is an important factor governing interfilament spacing.

The ability to model the measured electrochemical potentials from various regions of the sarcomere at varying lattice spacings demonstrates the applicability of Donnan equilibrium theory to polyelectrolyte systems. The relationship of the potential to interaxial distance argues strongly for the role of electrostatic repulsive forces derived from the filament charges in the stability of the A-band liquid-crystalline lattice.

We thank Phillip W. Brandt of Columbia University for the use of his FORTRAN programs, David W. Maughan of the University of Vermont for allowing us the use of unpublished work, Ernest Amatniek of Columbia University for his technical advice, and Raymond J. Hawkins for insightful discussions.

This work was supported by grants from the National Institutes of Health (5R01 AM15876) and the Equitable Life Assurance Society of the United States through the Insurance Medical Scientist Scholarship Fund.

Received for publication 20 November 1985 and in final form 18 November 1986.

REFERENCES

Aldoroty, R. A., and E. W. April. 1981. Microelectrode measurements of Donnan potentials within crayfish striated muscle. *J. Gen. Physiol.* 78:11a. (Abstr.)

Aldoroty, R. A., and E. W. April. 1982. Microelectrode measurement of A-band Donnan potentials as a function of relative volume. *Biophys. J.* 37 (2, pt. 2):121a. (Abstr.)

Aldoroty, R. A., and E. W. April. 1984. Donnan potentials from striated muscle liquid crystals: A-band and I-band measurements. *Biophys. J.* 46:769–779.

Aldoroty, R. A., and E. W. April. 1985. Donnan potentials generated by the surface charge of striated muscle filaments. *J. Electrochem. Soc.* 132:127C.

Aldoroty, R. A., N. B. Garty, and E. W. April. 1985. Donnan potentials from striated muscle liquid crystals: sarcomere length dependence. *Biophys. J.* 47:89–96.

April, E. W. 1969. The effects of tonicity and ionic strength on tension and filament lattice volume in single muscle fibers. Ph.D. Thesis. Columbia University, New York. 44–46.

April, E. W. 1975*a*. Liquid crystalline characteristics of the thick filament lattice of striated muscle. *Nature* (Lond.). 257:139–141.

April, E. W. 1975*b*. The myofilament lattice: studies on isolated fibers. IV. Lattice equilibria in striated muscle. *J. Mechanochem. Cell Motil.* 3:111–121.

April, E. W. 1978. Liquid crystalline contractile apparatus in striated muscle *ACS (Am. Chem. Soc.) Symp. Ser.* 74:248–255.

April, E. W. 1980. Interfilament spacing changes in striated muscle during cross-bridge interaction. *Fed. Proc.* 39:1963.

April, E. W., and R. A. Aldoroty. 1986. Donnan potentials generated by the surface charge on muscle filaments. *In* Electrical Double Layers in Biology. M. Blank, editor. Plenum Publishing Corp., New York. 287–300.

April, E. W., and D. W. Maughan. 1986. Active force as a function of filament spacing in crayfish skinned muscle fibers. *Pfluegers Arch. Eur. J. Physiol.* 407:456–460.

April, E. W., and J. Schreder. 1979. Role of osmotic forces in the myofilament lattice stability in striated muscle. *Biophys. J.* 25(2, Pt. 2):18a. (Abstr.)

April, E. W., and D. Wong. 1976. Non-isovolumic behavior of the unit cell of skinned striated muscle fibers. *J. Mol. Biol.* 101:107–114.

April, E. W., P. W. Brandt, and G. F. Elliott. 1971. The myofilament lattice: studies on isolated fibers. I. The constancy of the unit cell volume with variations in sarcomere length in a lattice in which the thin-to-thick myofilament ratio is 6:1. *J. Cell Biol.* 51:72–82.

April, E. W., P. W. Brandt, and G. F. Elliott. 1972. The myofilament lattice: studies on isolated fibers. II. The effects of osmotic strength, ionic concentration, and pH on the unit-cell volume. *J. Cell Biol.* 53:53–65.

Bartels, E. M., and G. F. Elliott. 1980. Donnan potential measurements in the A- and I-bands of cross-striated muscles and calculation of the fixed charge on the contractile proteins. *J. Musc. Res. Cell. Motil.* 1:452.

Bartels, E. M., and G. F. Elliott. 1981*a*. Donnan potentials from the A and I bands of skeletal muscle, relaxed and in rigor. *J. Physiol. (Lond.)*. 317:85P–86P.

Bartels, E. M., and G. F. Elliott. 1981*b*. Donnan potential measurements in the A and I band regions of barnacle muscle fibers under a variety of physiological conditions. *J. Gen. Physiol.* 78:12a. (Abstr.)

Bartels, E. M., and G. F. Elliott. 1982. Donnan potentials in rat muscle differences between skinning and glycerination. *J. Physiol.* (Lond.). 327:72–73P.

Bartles, E. M., and G. F. Elliott. 1985. Donnan potentials from the A- and I-bands of glycerinated and chemically skinned muscles, relaxed and in rigor. *Biophys. J.* 48:61–76.

Bartels, E. M., T. D. Bridgman, and G. F. Elliott. 1980. A study of the electrical changes on the filaments in striated muscle. *J. Musc. Res. Cell. Motil.* 1:194.

Benedek, G. B., and F. M. H. Villars. 1979. Physics with Illustrative Examples of Medicine and Biology. Vol. 3. Electricity and Magnetism. Addison-Wesley Publishing Co., Inc., Reading, MA. 134–135.

Blinks, J. R. 1965. Influence of osmotic strength on cross-section and volume of isolated single muscle fibers. *J. Physiol.* (*Lond.*). 177:42–59.

Chichibu, S. 1961. Electrical properties of glycerinated crayfish muscle fiber. *Tohoku J. Exp. Med.* 73:170–179.

Collins, E. W., and C. Edwards. 1971. Role of Donnan equilibrium in the resting potentials in glycerol-extracted muscle. *Am. J. Physiol.* 221:1130–1133.

Dewey, M. M., S. F. Fan, and P. R. Brink. 1982. Measurement of Donnan potentials in relaxed and contracted muscle. *Biophys. J.* 37(2, Pt. 2):125a. (Abstr.)

Elliott, G. F. 1973. Donnan and osmotic effects in muscle fibers without membranes. *J. Mechanochem. Cell Motil.* 2:83–89.

Elliott, G. F., and E. M. Bartels. 1982. Donnan potential measurements in extended hexagonal polyelectrolyte gels such as muscle. *Biophys. J.* 38:195–199.

Elliott, G. F., and E. M. Rome. 1969. Liquid crystalline aspects of muscle fibers. *Molec. Cryst. Liq. Cryst.* 5:647–650.

Elliott, G. F., G. R. S. Naylor, and A. E. Woolgar. 1978. Measurements of the electric charge on the contractile proteins in glycerinated rabbit psoas using microelectrode and diffraction effects. *Colston Pap.* 29:329–339.

Elliott, G. F., E. M. Bartels, P. H. Cooke, and K. Jennison. 1984. Evidence for a simple Donnan equilibrium under physiological conditions. *Biophys. J.* 45:487–488.

Elliott, G. F., E. M. Bartels, and R. A. Hughs. 1986. The myosin filament: charge amplification and charge condensation. *In* Electrical Double Layers in Biology. M. Blank, editor. Plenum Publishing Corp., New York. 277–285.

Hawkins, R. J., and E. W. April. 1981. X-ray measurements of the bulk modulus of the myofilament liquid crystal in striated muscle. *Mol. Cryst. Liq. Cryst.* 75:211–216.

Hawkins, R. J., and E. W. April. 1983. The planar deformation behavior of skinned striated muscle fibers. *Mol. Cryst. Liq. Cryst.* 101:315–328.

Hinke, J. A. M. 1980. Water and electrolyte content of the myofilament phase in the chemically skinned barnacle fiber. *J. Gen. Physiol.* 75:531–551.

Kawai, M., and P. W. Brandt. 1976. Two rigor states in skinned crayfish single muscle fibers. *J. Gen. Physiol.* 68:267–280.

Maughan, D. W., and R. E. Godt. 1979. Restoration of constant volume behavior to skinned skeletal muscle fibers. *Biophys. J.* 25(2, Pt. 2):116a. (Abstr.)

Maughan, D. W., and R. E. Godt. 1981. Radial forces within muscle fibers in rigor. *J. Gen. Physiol.* 77:49–64.

Millman, B. M., and K. Wakabyashi. 1979. Shrinking of the muscle filament lattice in polymeric solutions. *Biophys. J.* 25(2, Pt. 2):111a. (Abstr.)

Naylor, G. R. S. 1977. X-ray and microelectrode studies of muscle. Ph.D. Thesis. The Open University, England.

Naylor, G. R. S. 1981. On the average electrostatic potential between the filaments in striated muscle and its relation to a simple Donnan potential. *Biophys. J.* 38:201–204.

Naylor, W. G., and C. R. Merrillees. 1964. Some observations on the fine structure and metabolic activity of normal and glycerinated ventricular muscle of toad. *J. Cell. Biol.* 22:533–550.

Naylor, G. R. S., E. M. Bartels, T. D. Bridgman, and G. F. Elliott. 1985. Donnan potentials in rabbit psoas muscle in rigor. *Biophys. J.* 48:47–59.

Ostle, B., and R. W. Mensing. 1975. Statistics in Basic Research: Basic Concepts and Techniques for Research Workers. The Iowa State University Press, Ames, IA. Chap. 6.

Overbeek, J. ThG. 1956. The Donnan equilibrium. *Prog. Biophys. Biophys. Chem.* 6:57–84.

Pemrick, S. M., and C. Edwards. 1974. Differences in the charge distribution of glycerol-extracted muscle fibers in rigor, relaxation, and contraction. *J. Gen. Physiol.* 64:551–567.

Scordilis, S. P., H. Tedeschi, and C. Edwards. 1975. Donnan potential of rabbit skeletal muscle myofibrils. I. Electrofluorochromometric detection of potential. *Proc. Natl. Acad. Sci. USA.* 72:1325–1329.

Segal, I. H. 1968. Biochemical Calculations: How to Solve Mathematical Problems in General Biochemistry. 2nd Ed. John Wiley & Sons, Inc., New York. 32–46.

van Harreveld, A. 1936. A physiologic solution for freshwater crustaceans. *Proc. Soc. Exp. Biol. Med.* 34:428–432.

Weast, R. C., ed. 1972. Handbook of Chemistry and Physics. 53rd Ed. The Chemical Rubber Company, Cleveland, OH. D120.

Wilson, E. B. 1952. An Introduction to Scientific Research. McGraw-Hill Book Co., New York. 272–274.